Applied Geochemistry 78 (2017) 105–115

Contents lists available at ScienceDirect

Applied Geochemistry

journal homepage: www.elsevier.com/locate/apgeochem

Evidence of trace element emission during the combustion of sulfide-bearing metallurgical slags☆

Svetlana Borisovna Bortnikova [a], Vladimir Vladimirovich Olenchenko [a], Olga Lukinichna Gaskova [b, c], Konstantin Ivanovich Chernii [d], Anna Yurevna Devyatova [a, c, *], Dmitrii Olegovich Kucher [a]

[a] Trofimuk Institute of Petroleum Geology and Geophysics, Siberian Branch of the Russian Academy of Sciences, Koptug ave. 3, Novosibirsk 630090, Russia
[b] Sobolev Institute of Geology and Mineralogy Siberian Branch of the Russian Academy of Sciences, Koptug ave. 3, Novosibirsk, Russia, 630090
[c] Novosibirsk State University, Pirogova Str. 2, Novosibirsk 630090, Russia
[d] LLC "Recycling", Unosty Str., 17, Belovo, Kemerovo region, 652600, Russia

ARTICLE INFO

Article history:
Received 27 September 2016
Received in revised form
22 December 2016
Accepted 22 December 2016
Available online 24 December 2016

Keywords:
Metallurgical slags
Combustion
Condensates
Experimental study
Geophysical and chemical modeling

ABSTRACT

The present study shows the results of field and laboratory studies of trace element transfer from waste heaps of metallurgical slags (Kemerovo region, town of Belovo). Temperature anomalies were observed, with high temperatures up to 81.2 °C on the top of the heap. A visual geophysical model of the inner parts of the heap with contrasting resistivity zones was obtained using the electrical resistivity tomography (ERT) method, and quantitative characteristics were derived. Dry and frozen slag zones were characterized by resistivity of 50–500 Ohm·m. The resistivity of wet slag varied from 5 to 10 Ohm·m for slag with low humidity of 1–2 Ohm·m for slag saturated with highly mineralized solutions. The local anomaly of extremely low resistivity (0.3–0.5 Ohm·m) might be associated with a combustion centre or high pore solutions TDS. Basic major elements (Ca, Mg, K, Na, Si, and Al), metals (Cu, Zn, Pb, and Cd) and anionic elements (As, Sb, and V) were determined in gas condensates *in situ*. The most volatile elements were basic elements: Ca > Cu > Mg > Na > Mn > Fe, Zn. Lower concentration in the condensates was determined for Si > K > As > Sr > Al > V and Pb, Ba, La were also found. The observed mineral paragenetic sequences were primary minerals of barite-polymetallic ores and sphalerite concentrate, high-temperature minerals formed during pyrometallurgical processing and/or permanent combustion of the heap surface, efflorescence minerals formed by atmospheric oxidation accelerated by acid steam condensation. An experimental investigations using stepwise and 500 °C heating of the same samples were performed to compare the elements that were released into the gas phase *in situ* and off-site.

1. Introduction

According to previous studies of heavy metal emission from main anthropogenic sources into the atmosphere, all industry plants as well as fuel combustion, transport and other types of human activity lead to the global dispersion of chemical elements throughout the environment (Nriagu and Pacyna, 1988; Pacyna and Pacyna, 2002). According to the World Health Organization, air pollution is the major cause of cancer diseases and significantly affects the level of cardiovascular illness. In the modern world, much attention is focused on studying the effects of coal combustion at thermal power stations because coal retains an important position as a world energy source (Linak and Wendt, 1993, 1994; Querol et al., 1995; Xu et al., 2003; Liu et al., 2010). The combustion of traditional and nonconventional fuels, biomasses, and municipal wastes affect the regional climate, biochemical cycles of elements, and human health (Nriagu, 1979; Pacyna, 1984, 1986; Ostromogilsky et al., 1987; Lighty et al., 2000). Multi-models of aerosols have recently been evaluated (Pan et al., 2015); methods for gas analyses as well as the accuracy of gas analyses are increasingly improved (Zhang and Chen, 2015). Recent studies have

☆ This paper has been recommended for acceptance by Prof. M. Kersten.

* Corresponding author. Koptug ave. 3, Novosibirsk 630090, Russia.
E-mail addresses: BortnikovaSB@ipgg.sbras.ru (S.B. Bortnikova), OlenchenkoVV@ipgg.sbras.ru (V.V. Olenchenko), Gaskova@igm.nsc.ru (O.L. Gaskova), k.cherny@pinsapogold.com (K.I. Chernii), devyatovaay@ipgg.sbras.ru (A.Y. Devyatova), KucherDO@ipgg.sbras.ru (D.O. Kucher).

http://dx.doi.org/10.1016/j.apgeochem.2016.12.016
0883-2927/

focused on the special methods of sampling, stability of gas compounds and accurate quantification of sulfur-containing compounds for the biogas and natural gas (Brown et al., 2015). As for sulfide ore tailings, physico-chemical mechanisms of substance oxidation leading to self-ignition of geological bodies have been studied, and methods of prediction and extinguishing sulfide fires have been proposed (Rosenblum and Spira, 1995; Cranney, 1997; Yang et al., 2003). An important aspect of this problem is the internal structure of the combustion sources and conductive fluids structures, but little is known about these structures. Li et al. (2004, 2005) undertook surveys of self-potential distributions to locate the spontaneous combustion of coal piles. Their results showed that there is a negative centre of the electrical potential distribution in the measurement area. The potential distribution is generated corresponding to the position of the heat source. Until recently, there are almost no studies concerning the chemical composition of man-made gas flows and the contents and species of elements migrating in the gas phase and aerosol condensate. Based on the ore formation theory, the lack of attention to these processes reflects the long-held belief concerning the insignificant role of the gas transfer of elements in hydrothermal processes (Krauskopf, 1964). It has been suggested that elements volatized and emitted in the vapor phase of the combustion of coal heaps are halogens (Cl, Br, and F), Hg, and partially B, Se, and I (Xu et al., 2003). As for a wider range of elements that could migrate with the gas phase, methods to assess the concentrations of elements in the air flow have only recently been proposed, primarily focusing on arsenic and selenium (Mestrot et al., 2009, 2011; Winkel et al., 2010).

As with any beginning, methodological difficulties for the collection of gas samples limit the ability to detect and study the elemental composition of gases and steam (Vriens et al., 2014). There is little research concerning the geochemistry of the elements in gas flow during sulfide tailing combustion. Recent studies have primarily focused on the volatility of metals in processes of coal burning (Verma et al., 2015; Zhang and Chen, 2015) municipal wastes (Chen et al., 2008; Liu et al., 2015a; Han et al., 2008; Liu et al., 2010), biomasses and tires (Raclavska et al., 2015).

The results suggest large-scale processes of element removal using steam in the form of the gas phase from a sulfide waste heap at an even ambient temperature (Bortnikova et al., 2016) and particularly during combustion. Unfortunately, the obtained data raise more questions than answers, thereby indicating the poor knowledge of these processes.

The goals of the present study is to conduct a complex investigation of burning slag heap directed on thermometric mapping, to determine the structure of combustion centre, to conduct geochemical experiments on collection and to analyze steam condensates. In this work, we applied condensate collection according to the practice of previous volcanology studies. The collection and analysis of condensates is widely used in studies of volcanic gases and emanations (Chevrier and Le Guern, 1982), first described by White and Waring (1963). We proposed that just as in volcanoes, the condensate composition in technogenic “fumaroles” reflects the composition of the steam.

2. Materials and methods

2.1. Study object

The slag heaps are located at the area of the Belovo zinc processing plant in the town of Belovo (Fig. 1a). The plant-extracted zinc was obtained after smelting from a sphalerite concentrate that was obtained from barite-sulfide ores mined at the Salair ore field (Sidenko et al., 2001; Bortnikova et al., 2011). This plant has operated since the 1930 s and processes sphalerite concentrates through pyrometallurgical smelting. The sphalerite concentrate was of low quality and contained high amounts of impurities because the ore comprised the fine-grained intergrowth of different sulfide minerals. Since the mid-1990 s, the plant has ceased operation. Approximately 1 million tons of slags containing significant amount of sulfuric acid remained in the plant area in heaps. The slag is a loose, coarse-grained material comprising silicate glass with inclusions of K-feldspar, olivine, spinel, alloys and sulfides (Sidenko et al., 2001). In addition, large amounts (approximately 20–25%) of fine-grained coke occur in the waste. The slag was stored in the heaps of approximately 15 m in height with a flat top and a steep slope (Fig. 1a). This waste was affected by the spontaneous ignition of the coke dust and subsequent burning of waste in the heaps.

Information about the composition of slags and drainage solutions had been provided in previous studies (Sidenko et al., 2001; Bortnikova et al., 2010, 2011). The substance combustion in this heap occurred for more than 20 years was extremely intense in the late 90 s, and then gradually faded. We used this heap as a model to identify inner combustion sources using electrotomography methods to determine the trace removal capabilities of the chemical elements in the gas phase.

2.2. Methods

Methods of investigation include the following:

- Thermometric mapping for identification of the location with high ground temperature reflecting inner heap combustion;
- Electrical resistivity tomography profiling through the heap and detailed profiles on the combustion area;
- Using the collection of steam condensates on waste heaps and solid sampling for chemical analyses and experiments;
- Laboratory experiments to evaluate the potential element migration with steam ranging in temperature from 150 to 500°C.

2.2.1. Field sampling

1. The temperature was measured using a IT-7 thermometer, and the measured temperature range from −50°C to +200°C (NPK “RELSIB”, Novosibirsk). Measurements were carried out in March, when an ambient air temperature varied about +2 ÷ +5 °C.
2. Electrical resistivity tomography (ERT) was performed along two profiles (Fig. 2). The first profile was 220 m in length and located along the flat heap top. The second profile was 115 m and located across the heap. Since the measurements were performed during the cold season, the top of the heap was partially frozen. The measurement step was 5 m. The measurements were performed using a SKALA-48 multielectrode electrical-survey instrument designed at the Laboratory of Electromagnetic Fields of the Institute of Petroleum Geology and Geophysics, Novosibirsk (Baikov et al., 2012), using an electrode connection sequence corresponding to the Schlumberger setup.
3. A set of gas condensate samples was collected on the burning slag heaps just after thermometric mapping. We used a standard method for condensate collection (Chevrier and Le Guern, 1982). Gas was passed sequentially through a Teflon funnel placed onto a steam output, then through a flexible Teflon tube connected to a bubbler trap cooled using cold water (Fig. 3a). Three samples were collected from three holes located at a distance of 3 m. Sidenko et al. (2001) determined elevated content of CO_2 in fumarolic gases at Belovo waste heaps and absence of sulfur

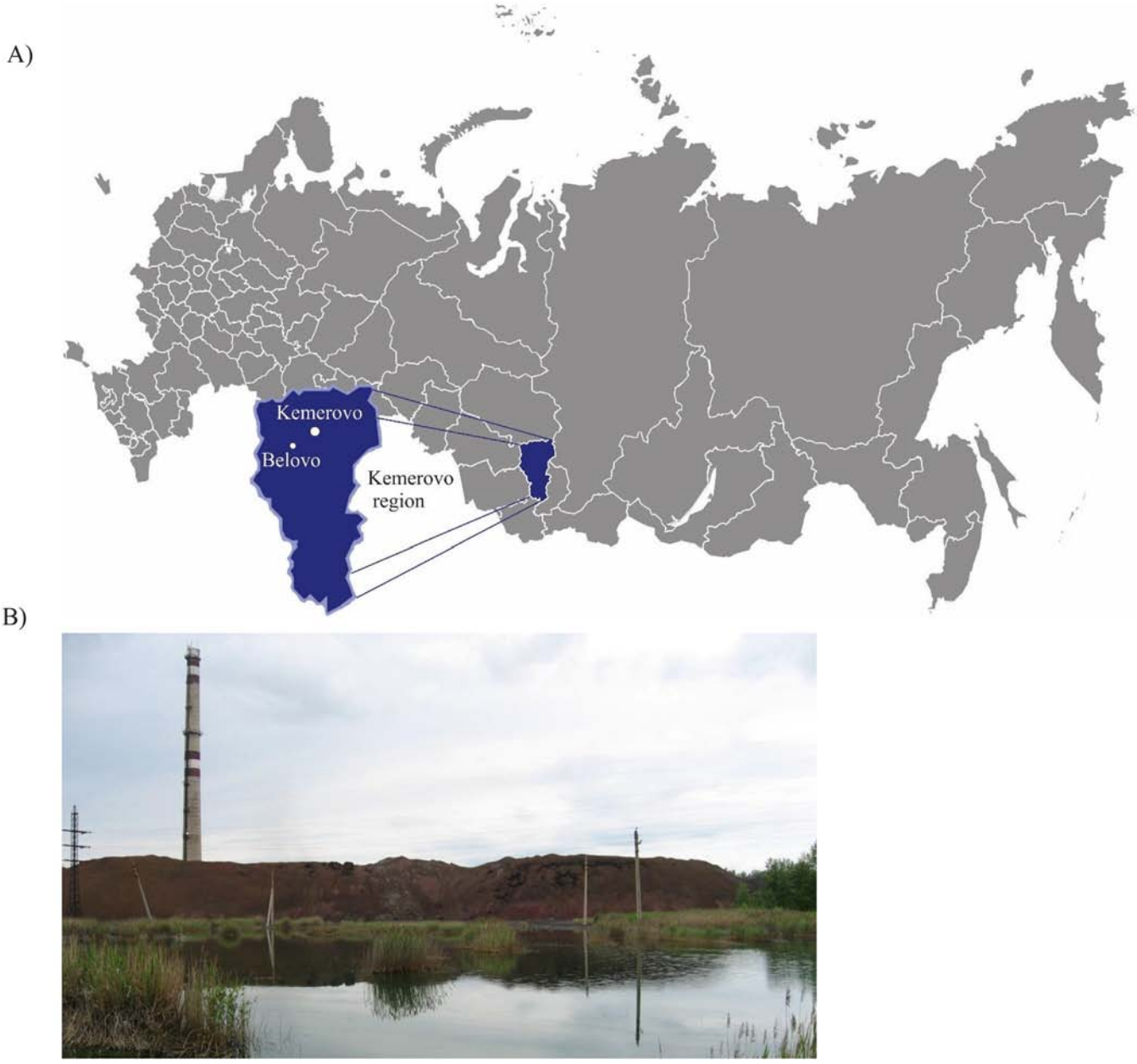

Fig. 1. **a**. Geographical location of the object of research. **b**. The general appearance of the slag heaps.

gases (SO_3 and H_2S). This may indicate that the main the cause of the self-burning process is residual coke dust.

4. Three large-volume samples of the slag were obtained for the laboratory experiments (Fig. 3b): black slag from the vicinities of the gas-emitting holes (sample B-1); slag with abundant efflorescent (white, blue and yellow crystals of Zn, Cu and Fe sulfates, sample B-2); and reddish-brown slag from a prospecting trench (sample B-3) (Fig. 4).

2.2.2. Geophysical data processing, laboratory analyses and experiments

1. The ERT results were previously processed, including the removal of erroneous data points on the curves (filtration). After the filtered data set was prepared, the 2D reverse problem of electrical prospecting was applied. The inversion was performed using the Res2DInv program (Loke, 2009). A robust inversion method with limited resistivity values of the model was applied. This constraint generates models with sharp interfaces between different regions with different resistivity values, but within each region, the resistivity value is almost constant. This method might be more suitable for the boundaries between areas with contrasting resistivities (Loke, 2009). As a result of the 2D inversion, geoelectric sections on profiles were constructed. According to the 3D inversion data, the resistivity distribution on different depths and volumetric geoelectric models were mapped.
2. A statistical analysis of the resistivity distribution was obtained, and based on the results, a 2-D inversion was conducted using the Past 3.1 Program. The “Mixture Analysis” tool of Program Past 3.1 facilitates the estimation of the parameters (mean value,

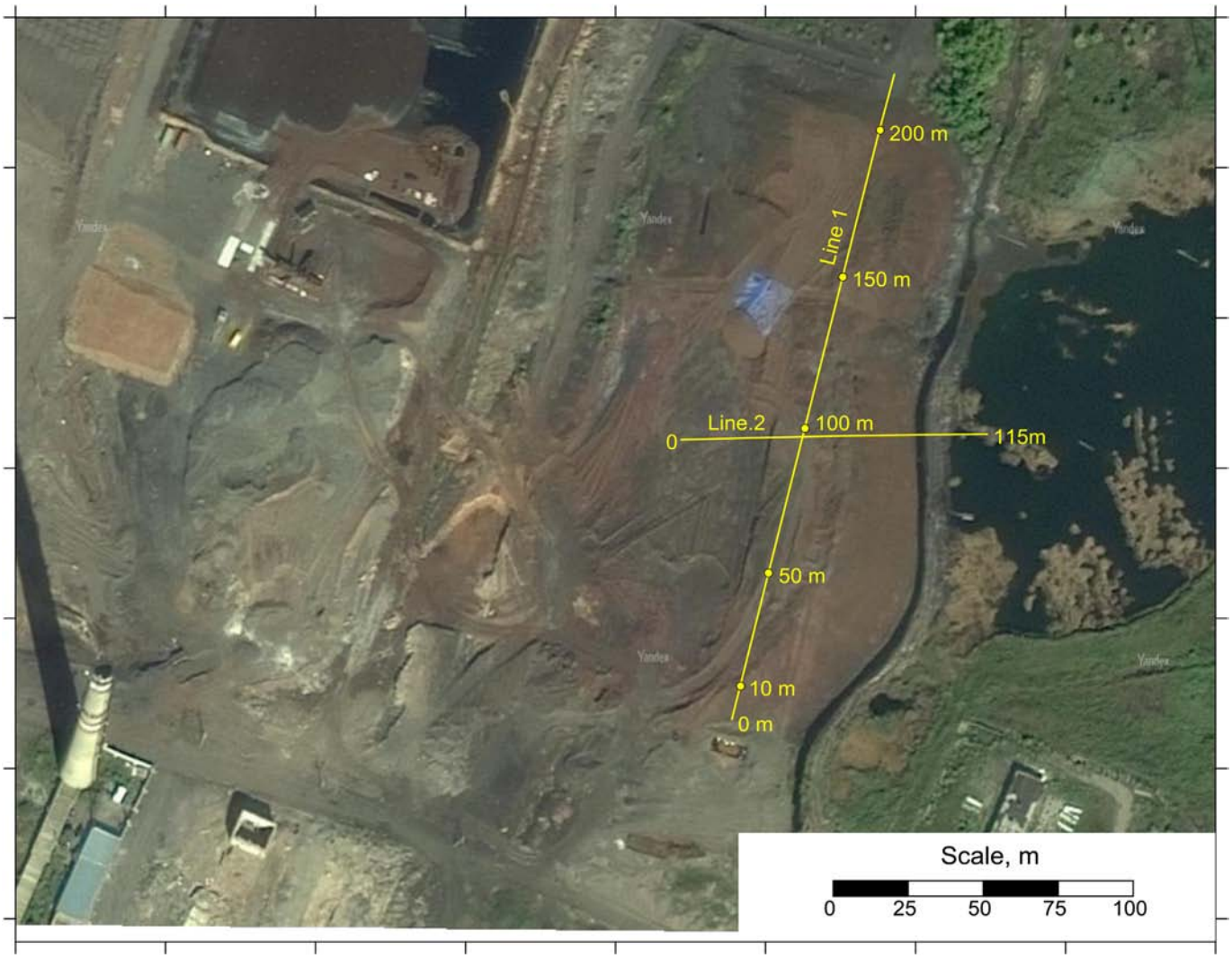

Fig. 2. ERT lines layout.

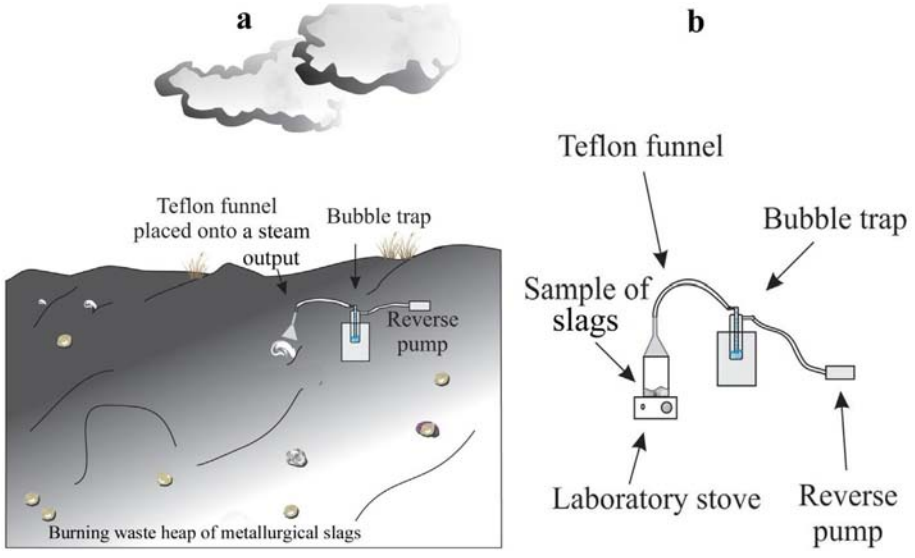

Fig. 3. Schematic of the experiments on condensate collection: (a) - on the burning slag heaps, (b) – in laboratory.

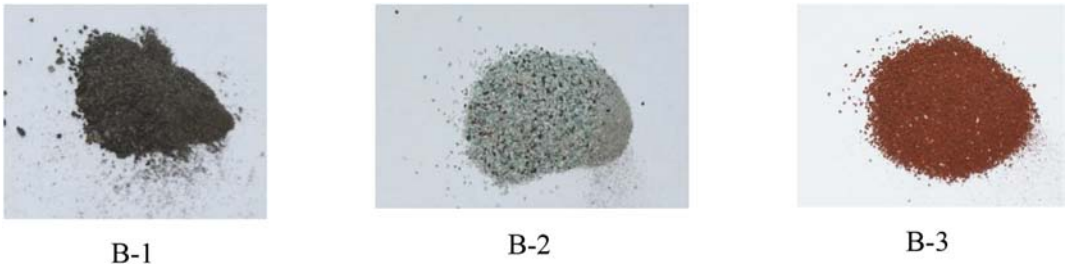

Fig. 4. Exterior slag samples for the experiments on calcination.

standard deviation, and specific gravity) of two or more linear normal distributions based on linear generalized sampling. The resistivity values were converted to logarithm values to approximate a normal distribution of resistivity, and after determination of the mean value and variance, the logarithms were converted to resistivity values.

3. Samples of the slag were sieved into +0.5 and −0.5 mm fractions. Experiments were conducted with the −0.5 mm fraction. The material was thoroughly homogenized after repeated remixing and quartering, and then 100 mg portions of each sample were used for the analyses.
4. The elemental composition of the samples was determined on pressed pellets of 30 mg mass using X RF with synchrotron radiation (Baryshev et al., 1986) at the VEPP-3 station at the Institute of Nuclear Physics SB RAS, Novosibirsk, Russia. Measurements were obtained at an activation energy of 30 keV using the method of internal standards; the measurement accuracy was ±15–20%. The resulting XRF spectra were processed using the AXIL program.
5. The mineral composition of the samples was identified through X-ray diffraction using a Dron diffractometer and automated peak search-match.
6. The experiment was conducted according to the following scheme. Ten grams from each of the samples were placed into a furnace in a ceramic crucible and heated at 150 °C for 1 day. Subsequently, the samples were weighed again and placed into the furnace at 250 °C for one day. The mineral composition was determined before the experiment.
7. To estimate the potential gaseous transport of trace elements, we collected condensates of steams that were released during sample heating using the following procedures. A total of 100 g of dry sample was placed into a quartz glass and heated on a laboratory stove. The gas that was separated from the sample was collected into a bubbler. Notably, at the beginning of the heating, some mist was observed on the glass walls, although the samples were dried to a constant weight at room temperature. Sample No. B-2 (with abundant efflorescent salts) evolved the largest amount of liquid. After the collection of the condensates from the dried samples, we added 50 ml of distilled water to each of the samples, followed by heating and collection of the condensates.
8. The collected condensates were analyzed through ICP-AES using an IRIS Advantage spectrometer (Thermo Jarell Ash Corporation, United States) at the Analytical Centre of the Institute of Geology and Mineralogy, Sb RAS.

3. Results and discussion

3.1. Thermometry

Based on the thermometric measurements, two narrow anomalies were identified in the northern and central parts of the heap with a ground temperature elevated to 81.2 C, indicating the top. Apparently, the combustion centres were located at these areas. In addition to high soil temperatures, burning inside the dump body indicated the presence of several small output streams of the vapor-gas mixture. A contrasting temperature drop was observed on the slopes of the heap (Fig. 5).

3.2. Electrotomography

The longitudinal resistivity section of the heap is shown in Fig. 6. In the upper part of the section to a depth approximately 10 m, the heap is characterized by high resistivity, reflecting its low humidity. At depths below 10 m, the heap resistivity was reduced to a few Ohm*m, reflecting the high TDS of the pore solutions. However, low resistivity was also observed in the centres of slag combustion. The local anomaly of low resistivity (less than 1 Ohm·m) in the interval of 120–135 m at a depth of 10–20 m has been associated with the combustion centre. The narrow channel of low resistivity most likely reflects the release of steam and gas jets from the combustion centre through the “fumarole”.

The electrical resistivity of the transverse cross-section (profile №2) varies from unit fractions to hundreds Ohm*m (Fig. 7). Both dry and frozen slag zones are characterized by a resistivity of 50–500 Ohm*m. The resistivity of the wet slag was determined based on the amount of pore water, showing salinity varying from 5 to 10 Ohm*m for the slag, with low humidity to 1–2 Ohm*m for the slag that was saturated with highly mineralized solutions. At a distance of 50–55 m, the profile crosses the section with a heated surface, within which snow has melted and steam was observed. On the geoelectric section under the heated surface, the local anomaly with extremely low resistivity (0.3–0.5 ohm*m) was observed, which is associated with a combustion centre.

A statistical analysis of the resistivity distribution in the medium based on the results of a 2-D inversion was conducted using the Past 3.1 Program. Generalized sampling was approximated with four linear normal distributions (Fig. 8).

Statistical analysis revealed the following slag complexes in the section, which differed according to the average resistivity: 1 - a small complex of slag with abnormally low resistivity (0.17 Ohm-m); 2 – slag with comparatively low resistivity (1.0 Ohm*m); 3 – slag with medium resistivity (8.3 Ohm*m); and 4 – slag with high resistivity (150 Ohm*m).

An extremely low resistivity (less than 15 Ohm*m) might reflect underground coal fires (Karaoulis et al., 2014; Revil et al., 1998; Schaumann et al., 2008). We can interpret anomalies with low resistivity as slag burning sources by analogy with underground coal fires.

Nevertheless, low values of resistivity could be associated with highly mineralized ground and pore waters (Revil et al., 1998; Olenchenko et al., 2016). TDS and the resistivity of groundwater were measured using special equipment. The TDS of the Belovo drainage solution was 25–30 g/L, and the conductivity was 10–14

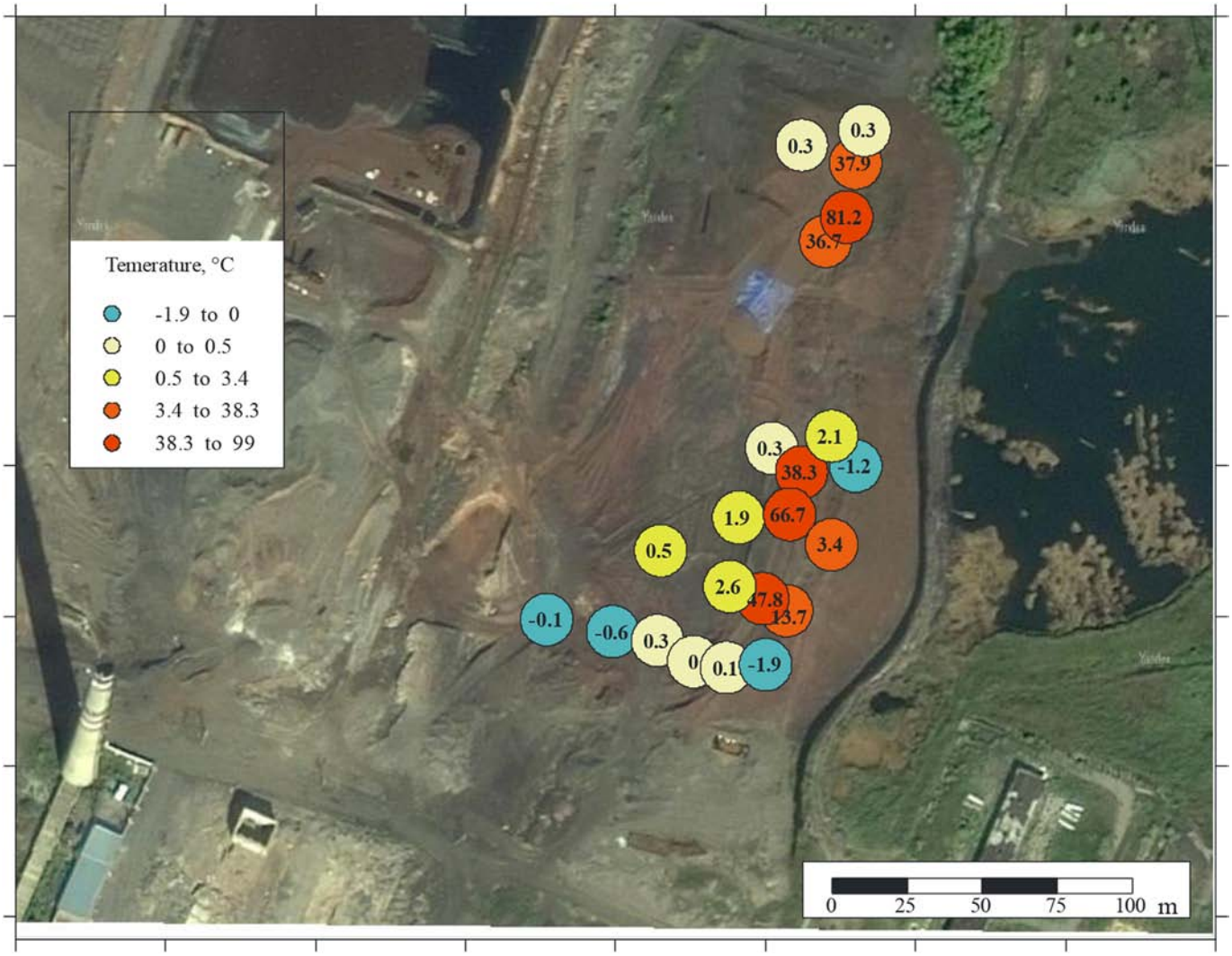

Fig. 5. Distribution of the temperature at a depth of 0.3 m in the Belovo waste heap.

mSm/cm (or 0.71–1.0 Ohm*m). According to the Archie Law, which associates the electrical resistivity of a rock to its porosity, the resistivity of the water that saturates its pores, and the fractional saturation of the pore space with the water are:

$$P = \frac{\rho_{g.w.}}{\rho_w},$$

where $\rho_{g.w.}$ is the resistivity of water-saturated rock;ρ_w is the resistivity of pore water.P is the relative resistance, depending on the

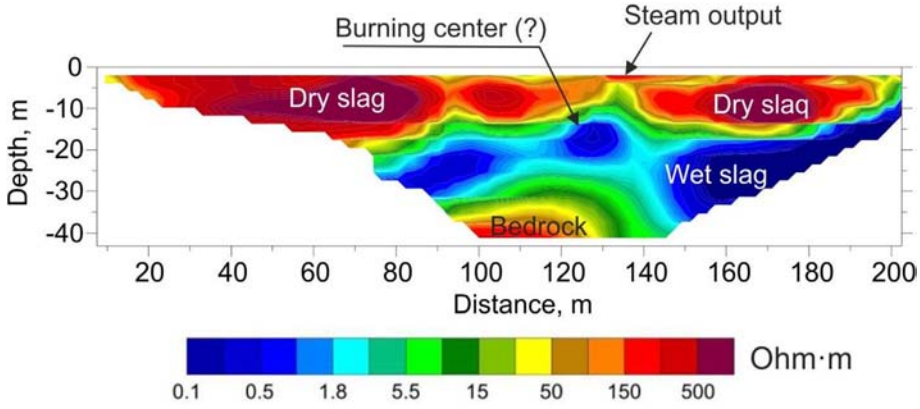

Fig. 6. Geoelectrical cross-section of profile 1.

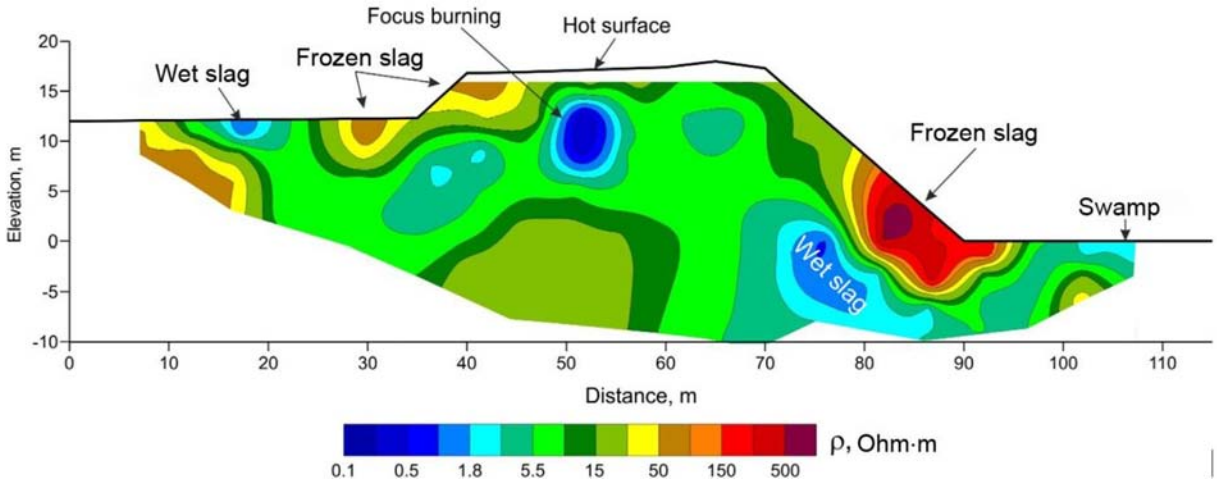

Fig. 7. Geoelectrical cross-section of Profile 2.

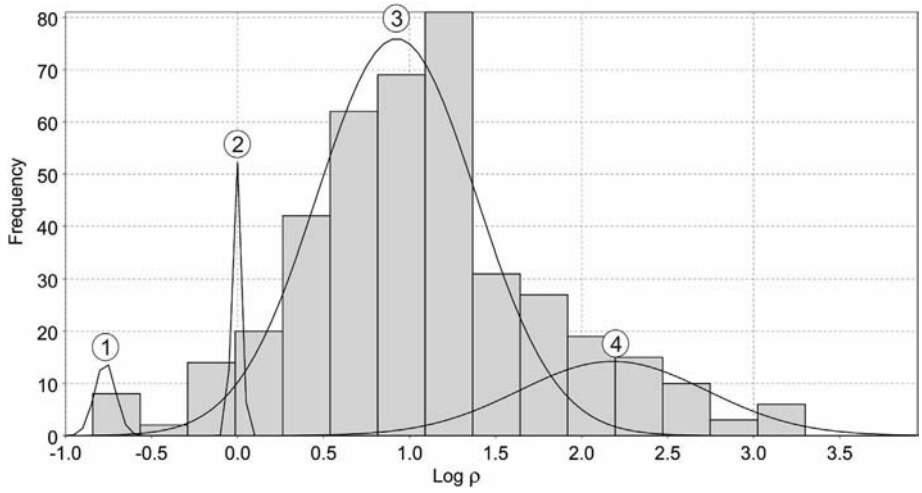

Fig. 8. The statistical distribution of the resistivity of slag substances according to the 2-D inversion approximated a four-bedded one-dimensional normal distribution. The modal value of the Log(SER) collection were as follows: No 1, −0.77 (0.17 Ohm*m); No 2, 0.0 (1.0 Ohm*m); No 3, 0.92 (8.3 Ohm*m); and No 4, 2.18 (150 Ohm*m).

volume of the pore space, associated with the porosity based on the following equation:

$$P = \frac{a}{n^m},$$

where *a* is a structural coefficient (0.5 < a >1);*n* is a porosity of rock; and.*m* is a cementation factor (1.3< *m* >2.3).

Taking pore solution resistivity ρw = 1/0 Ohm*m, slag porosity n = 30% (slag is approximated as loose sand), and structural coefficient a = 0.5, we calculated the resistivity of the water-saturated rock for a cementation factor *m* that was equal to 1.3 and 2.3. The value of 8.3 ohm*m was close to the resistivity of the largest group in sampling No. 3–8.1 Ohm*m (see Fig. 8).

Thus, resistivity of approximately 8 Ohm*m is typical for slag substances saturated with pore solutions with a TDS of 25–30 g/L. Anomalies of the lowest resistivity were observed under the heated surface, and a group of rocks with an average resistivity of 0.17 Ohm*m were interpreted as combustion centres. Species of elevated and high resistivity (40–500 Ohm*m) along the surface area were presented as frozen or dry slag substances.

3.3. Composition of steam condensates sampled in situ

A wide spectrum of elements was determined in the steam condensates (Table 1). Notably, condensates contained elements that migrated with a gas phase, including inert elements (Pb, Ba, and La). This result suggested that slag heap combustion leads to the intensive emission of elements through gas steams into the environment. Although the slag at the point of condensate collection appeared rather uniform, the condensate composition significantly varied, perhaps reflecting the fact that gases interact with slag substances of different geochemical and mineral compositions on the way to the surface.

According to the different mean element contents in condensates (and consequently volatilization), the elements can be divided into four groups.

1) Major elements (Ca > Cu > Mg > Na > Mn > Fe and Zn) whose concentration in the condensates is more than 1 mg/L. This group represents base elements of the slag.
2) Minor elements (Si > K > As) whose mean content ranges from 0.81 to 0.23 mg/L.

Table 1
Composition of steam condensates.

Elements	K-1	K-2	K-3	Mean	Elements	K-1	K-2	K-3	Mean
	mg/L					μg/L			
Ca	4.6	12	3.7	6.8	Al	3.9	15	220	80
Mg	0.73	5.6	1.5	2.6	Pb	0.1	<0.1	12	4.0
Na	3.2	2.5	1.1	2.3	Cd	0.05	1.0	4.0	1.7
K	0.35	1.2	0.45	0.68	Rb	0.35	5.0	2.7	2.7
Si	0.61	0.023	1.8	0.81	Ba	8.2	7.1	1.0	5.4
Fe	0.12	3.2	0.08	1.1	As	67	580	45	230
Mn	0.065	0.021	5.4	1.8	Sb	0.58	3.0	<0.5	1.2
Sr	0.019	0.022	0.009	0.083	V	1.9	3.2	40	15
Cu	0.0016	14	0.85	5.0	La	5.0	0.21	<0.1	1.8
Zn	0.059	2.7	0.68	1.1					

3) Trace elements (Sr > Al > V) contained at concentrations ranging from 0.083 to 0.015 mg/L.
4) Rare trace elements (Cd, Sb, Pb, Rb, Ba, and La), released with steam at insignificant amounts. Nevertheless, this result suggested the migration of these elements in the gas phase.

Lithophile elements, namely those that readily combine with oxygen (Ca, Mg, Na, and Si), will form compounds such as $CaO_{(gas)}$ or $Ca{\cdot}H_2O_{(gas)}$. The chalcophile elements, namely those that have an affinity for sulfur (Cu, Zn, Fe), will carry-over as sulfide or sulfate species, although an investigation of volcanic gases showed that the main inorganic form of arsenic remains $As(OH)_{3(gas)}$ (Planer-Friedrich et al., 2006) in the case of an abundance of volatile As.

3.4. Calcination of the samples and collection of steam condensate in the laboratory

The geochemical and mineral composition of the samples in the present study significantly differed. Sample B-1 (black slag) is characterized by the greatest content of base rock-forming elements: SiO_2, TiO_2, Al_2O_3, MgO, K_2O, Na_2O, P_2O_5, and BaO (Table 2). The highest amount of chalcophile metals (Cu and Zn) was determined in sample B-2 (abundant efflorescent). Sample B-3 was the most ferric: the Fe_2O_3 content up to 57.1%.

Table 2
Concentration of elements in samples of slag, %.

Elements	B-1	B-2	B-3
SiO_2	22.6	1.25	12.5
TiO_2	0.73	0.13	0.39
Al_2O_3	6.2	0.22	3.8
CaO	2.9	0.34	6.26
Fe_2O_3	26.1	16	57.1
MnO	0.18	0.33	0.23
MgO	1.35	0.14	0.89
K_2O	2.79	0.6	0.92
Na_2O	1.94	0.34	1.19
P_2O_5	0.16	0.08	0.11
BaO	1.14	0.42	0.96
Cu	4.1	28.2	0.49
Zn	6.53	22.4	0.55
	ppm		
V	340	40	880
Sr	580	61	170
Rb	36	4,6	12
Pb	6100	1800	1700
Ni	170	2900	dl
Cr	92	80	300
Cd	120	55	35
Sb	200	190	940
As	1900	1400	3900
LOI	21.4	27.2	12.5

A detailed mineral composition of the studied samples is shown in Table 3.

The mineral paragenesis of black slag from the combustion zone (sample B-1) reflected a complex history of the transformation of the Salair sulfide ore from mining to processing and storage.

I Primary minerals of barite-polymetallic ore and sphalerite concentrate preserved during processing and subsequent storage (quartz, feldspar, pyrite, and sphalerite).
II High-temperature minerals formed through the pyrometallurgical processing of sphalerite concentrate and/or during the combustion of the heap:
- Sulfide berthierite $Fe(Sb,Bi)_2S$; wittichenite Cu_3BiS_3; and arsenide chloantite $(Ni,Co)As_3$ are minerals that have never been detected in the Salair ore; these rare sulfides and arsenide likely originated from interactions between the slag and H_2S released from sulfides when acidified (Somot and Finch, 2010).
- The formation of Fe-oxides, magnetite Fe_3O_4 and hematite Fe_2O_3, during combustion has been described previously in rocks associated with naturally burned coal-bearing spoil-heaps (Sokol et al., 1998; Žaček and Skála, 2015; Misz-Kennan et al., 2015). Pan et al. (2000) observed that hematite is produced from goethite at 350 °C.
- Oxides tridimite SiO_2 and mullite $Al_6Si_2O_{13}$ are also formed. Mullite is the high-temperature compound of Al_2O_3 and SiO_2, a typical component of technic products, such as shamotte.

III Secondary unstable minerals are formed from atmospheric oxidation accelerated through acid steam condensation (brochantite $Cu_4(SO_4)(OH)_6$, picropharmacolite $(Ca,Mg)_3(AsO_4)_2 \times 6H_2O$, hydrohonnessite $Na_6Fe_2(SO)_4(OH)_{16} \times 7H_2O$, jarosite $KFe^{(III)}{}_3(SO_4)_2(OH)_6$, liskeardite $(Al,Fe^{3+})_3(AsO_4)(OH)_6 \times 5H_2O$).

Sample B-2 represented water sulfates-crystalline hydrates with H_2O molecules up to 22, which formed on the heap surface under combination of atmospheric and acid gasses oxidation.

In contrast, sample B-3 primarily comprises Fe-oxides, gypsum and kaolinite. Thus, base elements (Ca, Mg, Na, K, Fe, Al, and Mn), metals (Cu, Zn, Pb, Co, and Ni), and metalloids (As, Sb, Bi, and V) formed their own minerals in B-1 and B-2 samples. However, these elements were observed as an isomorphic admixture in refractory Fe-oxides in sample B-3.

Experiments on stepwise heating confirmed high element concentrations in the gaseous phase and facilitated the estimation of the comparative mobility of the elements. After each of the stages of heating, we observed changes in both the mineral and chemical compositions of the slag (Table 4). Weight losses primarily reflected the separation of structural and adsorbed water.

Table 3
Mineral composition of slag samples.

B-1		B-2		B-3	
Mineral	Formula	Mineral	Formula	Mineral	Formula
Brochantite	$Cu_4(SO_4)(OH)_6$	Siderotile	$(Fe,Cu)SO_4 \cdot 5H_2O$	Hematite	Fe_2O_3
Berthierite	$Fe(Sb,Bi)_2S$	Gypsum	$CaSO_4 \cdot 2H_2O$	Goethite	FeOOH
Picropharmacolite	$(Ca, Mg)_3(AsO_4)_2 \times 6H_2O$	Bilinite	$FeF_2(SO_4)_4 \cdot 22H_2O$	Gypsum	$CaSO_4 \cdot 2H_2O$
Hydrohonnessite	$Na_6Fe_2(SO)_4(OH)_{16} \times 7H_2O$	Mirabilite	$Na_2SO_4 \cdot 10H_2O$	Magnetite	Fe_3O_4
Jarosite	$KFe^{(III)}{}_3(SO_4)_2(OH)_6$	Moorhouseite	$(Co,Ni,Mn)SO_4\ 6H_2O$	Kaolinite	$Al_2[Si_2O_5](OH)_4$
Quartz, tridimite	SiO_2	Melanterite	$FeSO_4 \cdot 7H_2O$		
K-feldspar	$KAlSi_3O_8$	Bianchite	$(Zn,Fe)SO_4 \cdot 6H_2O$		
Magnetite	Fe_3O_4	Bonattite	$CuSO_4\ 3H_2O$		
Hematite	Fe_2O_3	Stanleyite	$(V^{4+}O)(SO_4) \cdot 6H_2O$		
Pyrite	FeS_2	Thenardite	Na_2SO_4		
Sphalerite	ZnS	Chalcantite	$CuSO_4 \cdot 5H_2O$		
Liskeardite	$(Al,Fe^{3+})_3(AsO_4)(OH)_6 \times 5H_2O$	Osorizawaite	$Pb(Al,Cu,Fe)_3(SO_4)_2(OH)_6$		
Chloantite	$(Ni,Co)As_3$	Thometrekite	$PbCu_2(AsO_4)_2 \times 2H_2O$		
Wittichenite	Cu_3BiS_3	Osarizawaite	$PbCuAl_2(SO_4)_2(OH)_8$		
Mullite	$Al_6Si_2O_{13}$	Hidalgoite	$PbAl_3(AsO_4)(SO_4)(OH)_4$		
Lepidocrocite	γ-$Fe^{3+}O(OH)$	Thenardite	Na_2SO_4		
		Alocranite	As_8S_9		
		Hoethite	FeO(OH)		

Table 4
The scheme of the experiment and visual sample changes after heating.

Sample	Temperature, time	Loss/gain of weight	Visual changes
Б-1/1	150 °C, 24 h	−0.43 g	No
Б-2/1		−2.05 g	Poor adhesion of a 'cakes', the appearance of white flight
Б-3/1		−0.19 g	There were white particles
Б-1/2	250 °C, 24 h	−0.54 g	No
Б-2/2		−0.62 g	No
Б-3/2		−0.17 g	No
Б-1/3	350 °C, 24 h	−0.96 g	It has become gray with brown tint
Б-2/3		−0.75 g	The same
Б-3/3		−0.14 g	No
Б-1/4	500 °C, 12 h	+18.08 g	It has become gray with light brown tint
Б-2/4		+14.30 g	There were reddish-brown color
Б-3/4		+16.27 g	No

Variations in phase composition during the heating manifested as changes in the color, partial agglomeration, destruction of crystals or formation of new aggregates.

A significant weight increase of the samples after calcination at 500 °C was unexpected. Presumably, this effect reflected active hydration during the cooling-down of new-forming secondary phases. Screening experiments were conducted to substantiate this assumption. To this end, 2 g of each sample were heated for 6 h at 500°C in a muffler. Subsequently, the samples were rapidly cooled, weighed and placed in a desiccator for a day (Table 5). The samples were removed from the desiccator, weighed and left on the bench until the next day for weighing. Therefore, at the first weigh-in, a marked loss was observed, but after the storage of the samples under ambient conditions, a weight gain, in percentage terms less than in the first case, was observed because the samples cooled down in a desiccator and the absorption of water from the air already occurred through a cold substance.

Table 5
Results of additional experiments on sample heating.

Sample	Weight, g	Weight losses		Weight gain (hydration)	
		g	%	g	%
B-1	2.0461	−0.6715	32.8	+0.0155	0.76
B-2	2.1453	−0.7470	34.8	+0.1518	7.1
B-3	2.0416	−0.3002	14.7	+0.0145	0.71

In the next experiment (heating on the electric hot plate), we collected condensates of steams emitted at 500 °C. Intensive steam separation (judging by the amount of condensates in bubbler) proceeded with increasing temperature. Obviously, the steam was absorbed, and structural-connected water was separated during heating and destruction of mineral matrix. The amount and

Table 6
Composition of condensates in laboratory experiments, mg/L.

	Heating dry samples, 100 g			Addition 50 ml of water after heating		
	B-1/1	B-2/1	B-3/1	B-1/2	B-2/2	B-3/2
	2,5 ml	12,5 ml	1,0 ml			
Ca	6.4	25	14	6.2	1.3	3.0
Mg	1.8	32	2.3	1.2	0.79	0.49
Na	1.7	3.0	2.2	1.3	0.21	0.27
K	0.52	0.90	1.3	0.60	0.41	0.19
Fe	0.007	5.9	0.077	0.056	0.060	0.10
Al	0.013	5.3	0.14	0.16	0.16	0.15
Mn	0,013	7.8	0.011	0.023	0.074	0.016
Cu	0.0039	170	0.12	0.17	4.3	0.17
Zn	0.09	603	0.86	0.56	5.8	0.55
Pb	0.0005	0.14	0.0005	0.0068	0.005	0.003
Cd	0.0031	0.17	0.0011	0.0016	0.0045	<0.001
Ni	0.0059	0.16	<0.0005	0.45	0.078	<0.001
As	0.41	1.9	0.021	<0.0005	0.014	0.013
Sb	0.0022	0.03	0.0023	0.0026	<0.001	0.0021
Sr	0.0028	0.0054	0.001	0.013	0.0024	<0.001

composition of the collected condensates were different in investigated samples (Table 6). From sample B-1, we collected 2.5 ml of condensate containing basic cations (Ca, Mg, K, and Na), some metals (Fe, Al, Cu, and Zn) and anionic- elements (As and Sb). The maximal volume of condensate was released during the heating of B-2 sample, and this condensate was most saturated with chemical elements. Sample B-3, representing (hydro)oxides (hematite, goethite, and magnetite), had a minimal amount of condensate, and the element concentrations in this sample were much lower than those in B-2 condensate. In general, there was a clear tendency to increase the quantity of the removal elements with increasing degree of oxidation and alteration of substances.

Evaluation of the comparative element volatility (coefficient of volatility – K_{vol}) was realized based on the amount of a particular element in the solid and in the condensate:

$$K_{vol} = \mathrm{Log}\left(\frac{C_{solid}}{10} \Big/ \frac{C_{cond} \times V_{cond}}{1000}\right),$$

where C_{solid} is concentration of the element in solid sample, ppm;C_{cond} is concentration of the same element in condensate, mg/L; V_{cond} is volume of the condensate, ml.

Thus, the lower the K_{vol} is, the higher the element volatility. Orders of the element volatility for the studied samples are shown on in Fig. 9. General regularity showed the low volatility of the elements in B-1 and B-3 samples compared with the B-2 sample. Thus, Fe and Pb were most inert elements in all the samples. Nevertheless, the K_{vol} for these elements as well as for Mn, Cu, Zn, and Cd was four orders of magnitude less in sample B-2 than in samples B-1 and B-3, suggesting a significant lower volatility of the elements in samples B-1 and B-3. Obviously, this effect was determined based on differences in the modes of the occurrences of the elements in the samples.

The condensates examined in the second part of the experiment (with addition of water) also contained high trace element concentrations (see Table 6), although these amounts were slightly lower than those in the condensates from the “dry” samples, suggesting the potential transport of elements even during the simple evaporation of water from the heap surface.

4. Conclusions

In the present study, the slag heap burning process was described, the structure of combustion zone was detected using geophysical methods and the composition of gas condensates was analyzed in detail. The main conclusions are summarized.

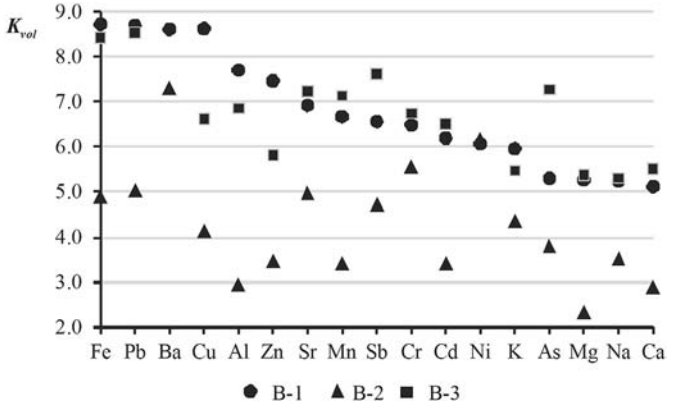

Fig. 9. Volatility coefficient of the elements at steam release in the laboratory experiment.

1. Narrow temperature anomalies were observed in the northern and central parts of the Belovo slag heap with a high temperature up to 81.2 °C on the top of the heap. This hot spot indicates a potential combustion centre at a certain depth. Spontaneous burning of coke dust is the cause of heating that was enhanced by a significant amount of dumped sulfuric acid.
2. The inner part of the heap has contrasting resistivity zones that were obtained by the ERT method. The local anomaly with resistivity less than 1 Ohm·m at a depth of 10–20 m can be related to the combustion centre accompanied by a low resistivity fumarole channel. At a distance from hot spots, the local resistivity anomalies of 0.3–0.5 Ohm·m might be associated with zones saturated with high mineralized pore solutions. As a reference value we used high mineralized Belovo drainage solutions (TDS is 25–30 g/L) with resistivity of 0.71–1.0 Ohm·m. Dry and frozen slag zones are characterized by resistivity of 50–500 Ohm·m.
3. According to *mean* element concentrations in the gas condensates sampled *in situ*, basic elements of the slag Ca > Mg > Na and metals such as Cu > Mn > Fe, Zn are most volatile elements; lower concentrations were determined for Si > K > Al, most volatile ionic element is As; and Ba, Pb, Cd seem to be inert. A precaution should be done to prevent generalization due to the high heterogenity of slag substances.
4. Three typical samples from different combustion zones have been described. In general, B-1 sample consists of primary minerals of barite-polymetallic ores and refractory minerals formed during smelting or permanent combustion of the heap; B-2 sample is surface efflorescence minerals formed by atmospheric oxidation accelerated by acid steams condensation; and B-3 sample is the “final product of chemical weathering” that primary consists of oxides (57% Fe_2O_3 and 12.5% SiO_2) with gypsum and kaolinite, although higher As admixture was observed (0.39%).
5. An experimental heating of these samples and calculated coefficients of the volatility (K_{vol}) demonstrated the highest volatility of the B-2 sample elements. However, these fragile structures are released to the environment mainly as toxic seasonal flows and insignificantly due to the increase of near-surface summer atmospheric temperature. Order of the elements volatility of B-1 and B-3 samples are similar at first sight (high K_{vol} of Fe, Pb Ba and low coefficients of Ca, Mg, Na). Nevertheless, B-3 oxidized sample is characterized by lower volatility of As and Sb (<7 K_{vol} <8) despite their high content in the solid up to 3900 and 940 ppm respectively. This is important from an environmental point of view. Surprisingly, the volatility of Cu and Zn is higher in the same B-3 sample (<6 log K_{vol} <7) but their content is insignificant.

Acknowledgements.

We thank Ph.D. Natalia and Nikolai Yurkevich, Olga Saeva, and Maxim Kirillov for their help during field works, the Sergei Nechepurenko, Irina Nikolaeva, and Nadezhda Palchik for their help with geochemical and mineral analysis, R. Biteikina for help in the laboratory experiments. The financial support from the Russian Foundation for Basic Research (grant No. 14-05-00293) is gratefully acknowledged. The authors are indebted to M. Kersten, Yu. Manstein, and an anonymous reviewer for their important suggestions that greatly improved the manuscript.

Appendix A. Supplementary data

Supplementary data related to this article can be found at http://dx.doi.org/10.1016/j.apgeochem.2016.12.016.

References

Baikov, E.V., Belorodov, V.A., Manshteyn, A.K., Manshteyn, YuA., Panin, G.L., 2012. Electrotomography – in the geophysics [J]. Russ. Geophys. J. 6, 54–63.

Baryshev, V.B., Kulipanov, G.N., Skrinsky, A.N., 1986. Review of X-ray fluorescent analysis using synchrotron radiation. Nucl. Instru. Methods Phys. Res. Sec. A Accel. Spectrom. Detec. Assoc. Equip. 246 (1–3), 739–750.

Bortnikova, S.B., Manstein, YuA., Gaskova, O.L., Bessonova, E.P., Ermolaeva, N.I., 2010. Drainage water - mine tailings interaction: environmental risk and origin of secondary metal deposit [C]. WRI-13, Guanajuato, Mexico, 16–20 August. In: Barkle, P., Torres-Alvarado, I.S. (Eds.), Proceedings of the 13th Internat. Conference on Water-rock Interaction, pp. 9–14.

Bortnikova, S., Yu, Manstein, Saeva, O., Yurkevich, N., Gaskova, O., Bessonova, E., Romanov, R., Ermolaeva, N., Chernuhin, V., Reutsky, A., 2011. Acid mine drainage migration of Belovo zinc plant (South Siberia, Russia): multidisciplinary study. In: Scozzari, A., Mansouri), B. (Eds.), [M]. Water Security in the Mediterranean Region. An International Evaluation of Management, Control, and Governance Approaches. Springer, Netherlands, pp. 191–208.

Bortnikova, S.B., Devyatova, A.Yu, Shevko, E.P., Gaskova, O.L., Edelev, A.V., Ogudov, A.S., 2016. Trace element emission in gaseous phase from Komsomolsky sulfide tailings (Kemerovo region, Russia) [J]. Chem. Sustain. Dev. 24, 11–22.

Brown, A.S., van der Veen, A.M.H., Arrenius, K., Murugan, A., Culletion, L.P., Ziel, P.R., Li, J., 2015. Sampling of gaseous sulfur-containing compounds at low concentrations with a review of best-practice methods for biogas and natural gas application [J]. Trend Anal. Chem. 64, 42–52.

Chen, Y., Zhang, Y.G., Li, Q.H., Zhuo, Y.Q., Chen, C.H., 2008. Effects of chlorides on Cd partitioning and speciation in a simulated MSW incinerator [J]. Environ. Sci. 29 (5), 1446–1451.

Chevrier, R.M., Le Guern, F., 1982. Prélèvement et analyses des condensats de fumerolles sur volcans actifs: Soufri re de la Guadeloupe (1976-1977) et Pouzzoles et Vulcano (Italie) (1978). Bull. Volcanolo. 45 (3), 173–178.

Cranney, D.H., 1997. Assessing the hazards of blasting in reactive sulfide ores and the application of products to mitigate these hazards [C]. In: Proceedings of 28th Annual Institute on Mining Health, Safety and Research. American Institute of Mining and Metallurgy, Salt Lake City, pp. 111–117.

Han, J., Xu, M.H., Yao, H., Furuuchi, M., Sakano, T., Kim, H.J., 2008. Influence of calcium chloride on the thermal behavior of heavy and alkali metals in sewage sludge incineration [J]. Waste Manag. 28 (5), 833–839.

Karaoulis, M., Revil, A., Mao, D., 2014. Localization of a coal seam fire using combined self-potential and resistivity data [J]. Int. J. Coal Geol. 128, 109–118.

Krauskopf, K.B., 1964. The possible role of volatile metal compounds in ore genesis [J]. Econ. Geol. 59, 22–45.

Li B.R., Uchino K., Inoue M., Tanaka T., 2004. Location of spontaneous combustion in a coal waste pile by self-potential method [C], In: Proceedings of. 5th International Symposium on Mining Science and Technology (ISMST), 249 – 253.

Li B., Uchino K., Inoue M., 2005. Fundamental studies for detecting fire source of spontaneous combustion using the self-potential method - In situ measurement in a combusting coal waste pile [C], In: Proceedings of 8th International Mine Ventilation Congress: Brisbane, Australia, 2005(6), 345–348.

Lighty, J.S., Veranth, J.M., Sarofim, A.F., 2000. Combustion aerosols: factors governing their size and composition and implications to human health [J]. J. Air Waste Manag. Assoc. 50 (9), 1565–1618.

Linak, W.P., Wendt, J.O.L., 1993. Toxic metal emissions from incineration - mechanisms and control [J]. Prog. Energy Combust. Sci. 19 (2), 145–185.

Linak, W.P., Wendt, J.O.L., 1994. Trace-metal transformation mechanisms during coal combustion [J]. Fuel Process. Technol. 39 (1–3), 173–198.

Liu, J., Falcoz, Q., Gauthier, D., et al., 2010. Volatilization behavior of Cd and Zn based on continuous emission measurement of flue gas from laboratory-scale coal combustion [J]. Chemosphere 80 (3), 241–247.

Liu, J., Fu, J., Ning, X., Sun, S., Wang, Y., Xie, W., Huang, S., Zhong, S., 2015a. An experimental and thermodynamic equilibrium investigation of the Pb, Zn, Cr, Cu, Mn and Ni partitioning during sewage sludge incineration [J]. J. Environ. Sci. 35, 43–54.

Loke, M.H., 2009. Electrical Imaging Surveys for Environmental and Engineering Studies. A Practical Guide to 2-D and 3-D Surveys, RES2DINV Manual. http://www.abem.se/files/res/2dnotes.pdf (last visit 22.12.2015).

Mestrot, A., Uroic, M.K., Plantevin, T., Islam, M.R., Krupp, E.M., et al., 2009. Quantitative and qualitative trapping of arsines deployed to assess loss of volatile arsenic from paddy soil [J]. Environ. Sci. Technol. 43, 8270–8275.

Mestrot, A., Feldmann, J., Krupp, E., Hossain, M., Roman-Ross, G., et al., 2011. Field fluxes and speciation of arsines emanating from soils [J]. Environ. Sci. Technol. 45, 1798–1804.

Misz-Kennan, M., Fabiańska, M., Ciesielczuk, Ju, 2015. Thermal transformation of Waste Rocks at the Starzykowiec Coal Waste Dump, Poland//Coal and Peat Fires: a Global Perspective, vol. 3. Elsevier, Amsterdam, pp. 387–429.

Nriagu, J.O., 1979. Global inventory of natural and anthropogenic emissions of trace metals to the atmosphere [J]. Nature 279, 409–411.

Nriagu, J.O., Pacyna, J.M., 1988. Quantitative assessment of worldwide contamination of air, water and soil by trace metals [J]. Nature 333, 134–139.

Olenchenko, V.V., Kucher, D.O., Bortnikova, S.B., Gas'kova, O.L., Edelev, A.V., Gora, M.P., 2016. Vertical and lateral spreading of highly mineralized acid drainage solutions (Ur dump, Salair): electrical resistivity tomography and hydrogeochemical data [J]. Russ. Geol. Geophys. 57, 611–622.

Ostromogilsky, A.H., Kokorin, A.V., Vizhensky, V.A., et al., 1987. Monitoring of Background Contamination of the Environment [M] (Leningrad: Gidrometeoizdat).

Pacyna, J.M., 1984. Estimation of the atmospheric emissions of trace-elements from anthropogenic sources in Europe [J]. Atmos. Environ. 18 (1), 41–50.

Pacyna, J.M., 1986. Atmospheric trace elements from natural and anthropogenic sources. In: Toxic Metals in the Atmosphere [M]. J. Willey, N.Y.

Pacyna, E.G., Pacyna, J.M., 2002. Global emission of mercury from anthropogenic sources in 1995 [J]. Water Air Soil Pollut. 137 (1–4), 149–165.

Pan, Y., Zhu, R., Banerjee, S.K., Gill, J., Williams, Q., 2000. Rock magnetic properties related to thermal treatment of siderite: behavior and interpretation[J]. J. Geophys. Res. 105 (B1), 783–794.

Pan, W., Chao, Wu, Li Zi-jun, Yang Y.P., 2015. Self-heating tendency evaluation of sulfide ores based on nonlinear multi-parameters fusion [J]. Trans. Nonferrous Metals Soc. China 25 (2), 582–589.

Planer-Friedrich, B., Merkel, B., 2006. Volatile metals and metalloids in hydrothermal gases. Environ. Sci. Technol. 40, 3181–3187.

Querol, X., Fernandezturiel, J.L., Lopezsoler, A., 1995. Trace-elements in coal and their behavior during combustion in a large power-station [J]. Fuel 74 (3), 331–343.

Raclavska, H., Corsaro, A., Juchelkova, D., 2015. Effect of temperature on the enrichment and volatility of 18 elements during pyrolysis of biomass, coal, and tires [J]. Fuel Process. Technol. 131, 330–337.

Revil, A., Cathles, L.M., Losh, S., Nunn, J.A., 1998. Electrical conductivity in shaly sands with geophysical applications [J]. J. Geophys. Res. 103 (B10), 23,925–23,936.

Rosenblum, F., Spira, P., 1995. Evaluation of hazard from self-heating of sulfide rock [J]. Cim. Bull. 88 (989), 44–49.

Schaumann, G., Bernhard, S., Yu, C., 2008. Geophysical Investigation of Wuda Coal Mining Area, Inner Mongolia: Electromagnetics and Magnetics for Coal Fire Detection: UNESCO[M]. ERSEC Ecological Book Series. In: Spontaneous Coal Seam Fires, vol. 4. Mitigating a Global Disaster UNESCO Office Beijing, Beijing.

Sidenko, N.V., Giere, R., Bortnikova, S.B., Cottard, F., Palchik, N.A., 2001. Mobility of heavy metals in self-burning waste heaps of the zinc smelting plant in Belovo (Kemerovo Region, Russia) [J]. J. Geochem. Explor. 74 (1–3), 109–125.

Sokol, E., Volkova, N., Lepezin, G., 1998. Mineralogy of pyrometamorphic rocks associated with naturally burned coal-bearing spoil-heaps of the Chelyabinsk coal basin, Russia [J]. Eur. J. Mineral. 10, 1003–1014.

Somot, S., Finch, J.A., 2010. Possible role of hydrogen sulphide gas in self-heating of pyrrhotite-rich materials[J]. Miner. Eng. 23, 104–110.

Verma, S.K., Masto, R.E., Gautam, S., et al., 2015. Investigations on PAHs and trace elements in coal and its combustion residues from a power plant. Fuel 162, 138–147.

Vriens, B., Ammann, A.A., Hagendorfer, H., et al., 2014. Quantification of Methylated Selenium, Sulfur, and Arsenic in the Environment. Plos One 9 (7). No e102906.

White, D.E., Waring, G.A., 1963. Volcanic emanations. U.S. Geol. Surv. Prof. Pap. 440-K, 27p.

White D. E. and Waring G. A.,, L., Feldmann, J., Meharg, A., 2010. Quantitative and qualitative trapping of volatile methylated selenium species entrained through nitric acid [J]. Environ. Sci. Technol. 44, 382–387.

Xu, M., Yan, R., Zheng, C., Qiao, Y., Han, Y., Sheng, C., 2003. Status of trace element emission in a coal combustion process: a review[J]. Fuel Process. Technol. 85, 215–237.

Yang, Song-rong, Qiu, Guan-zhou, Hu, Yue-hua, 2003. Discussion on sulfides bio-oxidation mechanism [J]. Nonferrous Met. 55 (13), 80–83.

Žaček, V., Skála, R., 2015. Mineralogy of Burning-coal Waste Piles in Collieries of the Czech Republic [M]. Coal and Peat Fires: a Global Perspective, vol. 3. Elsevier, Amsterdam, pp. 109–159.

Zhang, M., Chen, L., 2015. Continuous underway measurements of dimethyl sulfide in seawater by purge and trap gas chromatography coupled with pulsed flame photometric detection[J]. Mar. Chem. 174, 67–72.